On the Influence of the non-WSSUS Condition in the Performance of IEEE 802.11-Based Channel Estimators for Vehicular Communications

Nicolás M. Ortega, Cesar A. Azurdia-Meza
Department of Electrical Engineering
Universidad de Chile
Santiago, Chile
{nortega, cazurdia}@ing.uchile.cl

Carlos A. Gutierrez
Faculty of Science
UASLP
San Luis Potosí, México
cagutierrez@ieee.org

F. M. Maciel-Barboza,
School of Mechanical and Electrical Eng.
Universidad de Colima
Colima, México
fermin_maciel@ucol.mx

***Abstract*—Measurement campaigns carried out in different propagation scenarios around the world have shown that the statistical properties of vehicular multipath radio channels are strongly non-stationary. However, in spite of its practical relevance, the impact of the channel's non-stationarities on the performance of the vehicular communication systems (VCS) has barely been investigated, and is therefore not fully understood. To increase the knowledge on such important subject, we present in this paper a comparative performance analysis of six channel estimation techniques for VCS based on the IEEE 802.11p Standard, namely, the Least Squares (LS), Spectral-Temporal Averaging (STA), Modified STA (MSTA), Constructed Data Pilots (CDP), Frequency Linear-Averaged Data Pilot (FLDP), and Time-Domain Reliable Frequency-Domain Interpolation (TRFI) estimation techniques. Using a novel simulation framework, we evaluate the estimators' performance in terms of their bit error rate (BER) for the case when the propagation channel fulfills the wide-sense stationary uncorrelated scattering (WSSUS) condition, and also for the case when such condition is not met. The obtained results show that the estimation techniques that apply a joint time-frequency interpolation (STA, FLDP, and TRFI) are considerably more sensible to the channel's non-stationarities than the techniques that only interpolate in the time domain (MSTA and CDP).**

***Index Terms*—Channel estimation, IEEE 802.11p, non-WSSUS channels, vehicular communications.**

I. Introduction

The use of vehicular communication systems (VCSs) for road safety, traffic control, navigation, and automation applications has gained a growing attention from both the industry and the scientific community [1], [2]. The VCS comprise information and communication technologies (ICT) that enable the transmission of information over wireless vehicle-to-vehicle (V2V) and vehicle-to-infrastructure (V2I) radio links. The term V2X communications has been coined as a general label for wireless communication system that connect vehicles among themselves and with the road infrastructure employing any form of V2V and V2I transmission links [3].

The IEEE 802.11p is the standard defined by the IEEE for short-range VCS. This standard, which was superseded in 2012 by the IEEE 802.11 Standard for wireless local area networks (WLANs), specifies the use of on orthogonal frequency division multiplexing (OFDM) for the physical layer (PHY) of V2X communication systems. This PHY-mode is an adaption of other modes of the 802.11 Standard (introduced as amendments 'a' and 'g') that were originally developed for fixed WLANs operating in quasi-static (time-invariant) indoor radio channels, where the users' mobility is a minor concern. The target operation scenarios of the original 802.11a/g PHY-modes are sharply different from the ones found in vehicular environments, where the users are moving rapidly.

To cope with the high mobility of the communicating vehicles, novel channel estimation techniques specifically tailored for the characteristics of V2X radio links must be conceived [4]. An obvious requirement for such estimation techniques is the ability of tracking the rapidly changing channel state information (CSI). This is important, because a slow tracking rate can result in outdated CSI snapshots that may compromise the detection process and the overall system's performance [5]. The challenge of designing proper channel estimators for VCS gets even more complex if one takes into account that recent empirical findings indicate that the vehicular multipath radio channel does not fulfill the wide-sense stationary uncorrelated scattering (WSSUS) condition. For example, empirical data obtained from measurement campaigns carried out independently in [6], [7] show that the WSSUS condition is valid only over short time intervals and frequency bandwidths.

The empirical evidence of the invalidity of the WSSUS condition has prompted a large amount of research activities aimed at the characterization of non-WSSUS V2X multipath radio channels. Consider, for example, the geometry-based stochastic models of non-WSSUS channels presented in [8]. In contrast, the impact of the channel's non-stationarities on the system performance has barely been investigated in the open literature. To shed some light on such an important subject, we present in this paper a comparative performance analysis of six channel estimation techniques for VCS based on the IEEE 802.11p Standard, namely, the Least Squares (LS) [9], Modified Spectral-Temporal Averaging (MSTA) [10], Constructed Data Pilots (CDP) [4], Spectral-Temporal Av-

eraging (STA) [11], Frequency Linear-Averaged Data Pilot (FLDP) [12], and Time-Domain Reliable Frequency-Domain Interpolation (TRFI) [13] estimation techniques. The first three techniques apply a time domain interpolation for CSI tracking and noise cancellation, whereas the later three apply a joint time-frequency interpolation. Following the novel framework presented in [10] for the simulation of non-WSSUS Rayleigh fading channels, we evaluate the BER performance of the six channel estimators. The estimators' BER was computed for the case when the propagation channel does not fulfill the WSSUS condition, and also for the case when such condition is met in order to provide a benchmark for assessing the impact of the channel's non-stationary characteristics.

The remainder of the manuscript is organized as follows. The signal model of the IEEE 802.11 packet is described in Section II. An overview of the six channel estimation techniques analyzed in this paper is provided in Section III. The simulation framework and the results of the performance comparison are presented in SectionIV. Section V concludes the paper with a summary of the principal findings.

II. Signal Model of the IEEE 802.11 Data Frame

A. System Description

For the analysis presented in this paper, we consider an OFDM signal characterized in the frequency-domain by the baseband-equivalent blockwise input-output relationship

$$Y_i(k) = H_i(k)\, X_i(k) + N_i(k), \qquad (1)$$

for $i = 0, 1, \ldots M$, and $k = 0, 1, \ldots, N-1$, where $X_i(k)$ and $Y_i(k)$ are the transmitted and received signals, respectively, for ith OFDM symbol (signal block) and the kth subcarrier, whereas $H_i(k)$ and $N_i(k)$ stand for the channel frequency response and the additive white Gaussian noise (AWGN) at the kth subcarrier and ith OFDM symbol, respectively.

Figure 1 shows a general block diagram of the OFDM receiver that will be considered for the analysis presented in this paper. In this diagram, uppercase letters stand for signals and systems in the frequency domain, while lowercase letters denote time-domain signals and systems. The ith OFDM symbol obtained after cyclic prefix removal is denoted by $y_i(n)$. This symbol is fed to a discrete Fourier Transform (DFT) block of $N = 64$ points (subcarriers). The output of this block is the signal $Y_i(k)$ defined in (1). The DFT is followed by the channel estimation and equalization blocks, which are of paramount importance for a robust data detection. The estimate of $H_i(k)$ generated by the channel estimation block is denoted by $\hat{H}_i(k)$. The received signal $Y_i(k)$ and the channel estimate $\hat{H}_i(k)$ serve as input parameters for the equalization block, and the output of this later block, $\hat{S}_{T,i}\,(k)$, serves as the input of the demodulation block.

The focus of this paper is on the propagation channel and the channel estimation blocks, which are highlighted in blue in Fig. 1. The channel estimation and demodulation blocks are interconnected in Fig. 1 as an open-loop system, although a closed-loop configuration can be implemented instead, depending on the particular characteristics of the channel estimation and equalization techniques, as it will be shown on Section III.

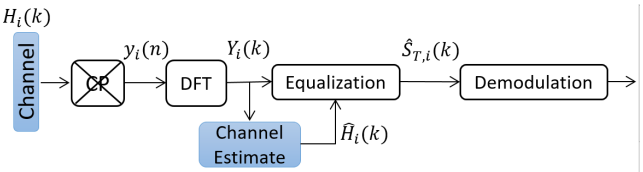

Fig. 1. Generic vehicular communication receiver.

B. 802.11p Preamble Structure

Figure 2 shows the structure of the preamble of an IEEE 802.11p packet. The preamble includes short and long training symbols. Short training symbols (t_1 to t_{10}) located at the beginning of every packet are used for synchronization. On the other hand, long training symbols T_1 and T_2 are used for subtle synchronization and channel estimation. $GI2$ stands for the combined double duration guard interval (GI) that precedes the two long training symbols. Following the signal model in (1), we will denote the transmitted (and received) OFDM signal block associated with the ten short training symbols by $X_0(k)$ (and $Y_0(k)$), while the two long training symbols will be represented by $X_1(k)$ and $X_2(k)$ ($Y_1(k)$ and $Y_2(k)$).

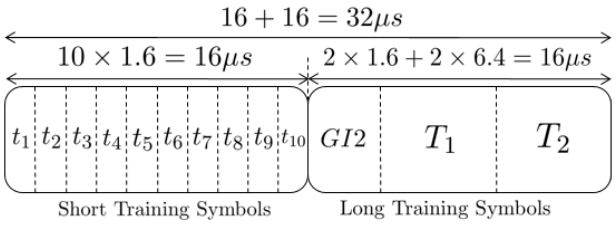

Fig. 2. IEEE 802.11p packet preamble.

Perfect synchronization between the transmitter and receiver is assumed, as the channel estimation techniques analyzed make use only of the long training symbols T_1 and T_2. The use of short training symbols t_1-t_{10} for synchronization purposes are beyond the scope of this paper.

C. Channel Frequency Response

The frequency response of the channel is modeled in this paper is in accordance with the non-WSSUS Rayleigh fading channel model that was recently proposed in [8]. Thereby, the discrete-time discrete-frequency channel frequency response $H_i(k)$ can be modeled by the combination of $\mathcal{L}$ multipath components as

$$H_i(k) = \sum_{\ell=1}^{\mathcal{L}} g_\ell \exp\{j[\theta_\ell + 2\pi\tau_\ell(i)[f_c - k\Delta f]\}, \qquad (2)$$

where $j^2 = -1$, Δf corresponds to the carrier separation, g_ℓ is the gain of the ℓth multipath component, and θ_ℓ is its corresponding phase shift. The carrier frequency is given by $f_c = C/\lambda$, where C stands for the speed of light and λ

is the wave-length of the transmitted signal; g_ℓ is modeled as a positive random variable (RV), and θ_ℓ is a uniformly distributed RV on $[-\pi, \pi)$. The time-varying propagation delays $\tau_\ell(t)$ of the multipath components are given as

$$\tau_\ell(t) = \frac{d_\ell^T + d_\ell^R}{C} - t\frac{f_\ell^D}{f_c}, \tag{3}$$

where d_ℓ^T denote the initial distance between the transmitter and a scattering object that generates the ℓth wave that arrives at the receiver, d_ℓ^R is the initial distance between such scatterer and the receiver, whereas

$$f_\ell^D = f_{\max}^T \cos(\theta_\ell^T - \gamma_T) + f_{\max}^R \cos(\theta_\ell^R - \gamma_R). \tag{4}$$

is the Doppler frequency shift caused by the vehicles' motion. In (4), $f_{\max}^p$ designates the maximum Doppler shifts due to the speeds of the transmitter ($p = T$) and receiver ($q = R$). The angles θ_ℓ^T and θ_ℓ^R are deterministic quantities that stand for the direction of motion of the transmitter ($p = T$) and receiver ($q = T$). Finally, the angle of arrival (AOA) θ_ℓ^T and angle of departure (AOD) θ_ℓ^R of the ℓth multipath signal are modeled by circular random variables [8]. For the simulation of the channel model defined in (2), we will follow the methodology proposed in [10]. The details on the implementation of the simulator will be omitted in this manuscript due to space limitations, but can be found in [10].

III. Channel Estimation Techniques

A. Least Squares Estimation

Least Squares (LS) estimator uses the long training symbols T_1 and T_2 to formulate a channel estimate, which is then used to equalize all data symbols in the packet [9]. The time-domain channel-corrupted symbols $T_1[n]$ and $T_2[n]$ are demodulated with a $N = 64$ -point DFT such that,

$$Y_1(k) = \sum_{n=0}^{N-1} T_1[n] e^{-jnk(2\pi/N)}, \quad k = 0, 1, \ldots, N-1, \tag{5}$$

$$Y_2(k) = \sum_{n=0}^{N-1} T_2[n] e^{-jnk(2\pi/N)}, \quad k = 0, 1, \ldots, N-1. \tag{6}$$

$Y_1(k)$ and $Y_2(k)$ denote the received frequency-domain symbols at subcarrier k for training symbols T_1 and T_2, respectively. Because the two training symbols are identical, the LS estimation for the channel frequency response is given by

$$\hat{H}_{LS}(k) = \frac{Y_1(k) + Y_2(k)}{X_1(k) + X_2(k)}. \tag{7}$$

This channel estimate is then applied to the incoming data symbols. The ith received data symbol $s_{R,i}[n]$, after CP removal, is demodulated and the frequency-domain symbol is given as

$$S_{R,i}(k) = \sum_{n=0}^{N-1} s_{R,i}[n] e^{-jnk(2\pi/N)}, \quad k = 0, 1, \ldots, N-1. \tag{8}$$

A zero forcing equalization process is employed, using the estimation obtained on equation (7), in order to obtain an estimate version of the ith transmitted symbol,

$$\hat{S}_{T,i}(k) = \frac{S_{R,i}(k)}{\hat{H}_{LS}(k)}. \tag{9}$$

The above described process is repeated for every data symbol on the package. It is clear that for a sufficiently long number of data symbols after the preamble, LS estimation is quickly outdated. Moreover, as we have discussed, V2X communications are characterized by highly dynamic environments, needing a constant updated CSI.

B. Spectral Temporal Averaging Estimation

Spectral Temporal Averaging (STA) estimation was originally presented in [11] as a technique that could fulfill the constant tracking requirement of V2X communications . It modifies the LS equalization of (9) as follows,

$$\hat{S}_{T,i}(k) = \frac{S_{R,i}(k)}{\hat{H}_{STA,i-1}(k)}, \tag{10}$$

where $\hat{H}_{STA,i-1}(k)$ is the previously estimated channel response. For the first data symbol of the package, $\hat{H}_{STA,i-1}(k)$ corresponds to the estimation done on (7). Equation (10) differs from (7) because now the channel estimate dynamically changes as a function of the symbol number i. To update the channel estimate, the channel is first estimated at each subcarrier such that

$$\hat{H}'_{STA,i}(k) = \frac{S_{R,i}(k)}{\hat{X}_i(k)}, \tag{11}$$

where $\hat{X}_i(k)$ is the ith determined symbol, obtained from a demapping operation on $\hat{S}_{T,i}(k)$ given from (10). Because the channel estimates in (11) are based on inherently unreliable data subcarriers, averaging in both frequency and time is employed to reduce the effects of noise and erroneous channel estimates caused by an incorrect determination of $\hat{X}_i(k)$. First, averaging in frequency is performed as

$$\hat{H}_{\text{STA,update}}(k) = \sum_{\lambda=-\beta}^{\lambda=\beta} \omega_\lambda \hat{H}'_{STA,i}(k+\lambda), \tag{12}$$

where ω_λ is a set of weighting coefficients that sums unity, and β is an integer parameter that determinate how many subcarriers are averaged in the frequency domain. After this frequency averaging has been completed, the new channel estimate $\hat{H}_{STA,i}(k)$ is computed as

$$\hat{H}_{STA,i}(k) = \left(1 - \frac{1}{\alpha}\right) \hat{H}_{STA,i-1}(k) + \frac{1}{\alpha} \hat{H}_{STA,\text{update}}(k), \tag{13}$$

where α is an updating parameter. This channel estimate is used to equalize the next data symbol, and the process is repeated until the packet is completely demodulated. For comparison reasons, and for the reasons explained in [11], in this manuscript we use $\omega_\lambda = 1/(2\beta+1)$ and $\alpha = \beta = 2$, resulting in an average of 5 adjacent sub carriers in each channel

estimation update. Note that if null carriers are adjacent, these are not considered and ω_λs are adjusted in order to sum unity. For example, if only 4 subcarriers are considered, as one of the original 5 subcarriers to be considered is null, ω_λ would be $1/4$ instead of $1/5$, as explained in [14].

C. Modified STA Estimation

As is shown [10], the frequency averaging of the STA techniques does not work very well on the non-WSSUS scenario. As a consequence, the authors of [10] proposed a modified version of the STA estimation. This was done by discarding the frequency averaging, such that the channel estimation is performed as

$$\hat{H}_{MSTA,i}(k) = \left(1 - \frac{1}{\alpha}\right) \hat{H}_{MSTA,i-1}(k) + \frac{1}{\alpha} \hat{H}'_{MSTA,i}(k), \tag{14}$$

where $\hat{H}'_{MSTA,i}(k)$ is obtained from (11). Because the MSTA estimation technique is completely based on the previously defined STA algorithm, it can be defined as a time-domain technique.

D. Constructed Data Pilots Estimation

Constructed Data Pilots (CDP) estimation is also based on the logic of the STA scheme, which dynamically updates the estimate of the channel, but integrating the existing correlation between two consecutively transmitted symbols [4]. First, the estimates in (10) and (11) are done. Then, two equalization processes are performed as follows

$$\hat{S}'_{C,i-1}(k) = \frac{S_{R,i-1}(k)}{\hat{H}'_{\text{CDP,i}}(k)}, \tag{15}$$

$$\hat{S}''_{C,i-1}(k) = \frac{S_{R,i-1}(k)}{\hat{H}_{\text{CDP},i-1}(k)}, \tag{16}$$

where $S_{R,i-1}(k)$ is the previously demodulated received symbol. Whereas $\hat{H}'_{\text{CDP},i}(k)$ in (15) is obtained from (11), while $\hat{H}_{\text{CDP},i-1}$ is the previous channel estimate. To update the channel estimate, a comparison process is performed. A demapping operation is performed both on (15) and (16), obtaining $\hat{X}'_{i-1}(k)$ and $\hat{X}''_{i-1}(k)$, respectively. As two time-adjacent data symbols should have a high correlation, if $\hat{X}'_{i-1}(k) \neq \hat{X}''_{i-1}(k)$, this implies that the demapping operation that gives $\hat{X}_i(k)$, and subsequently $\hat{H}'_{\text{CDP},i}(k)$, is wrong. Hence, the update on the channel estimate is done by $\hat{H}_{\text{CDP},i}(k) = \hat{H}_{\text{CDP},i-1}$, i.e., the previous channel estimate is maintained on the kth subcarrier. If $\hat{X}'_{i-1}(k) = \hat{X}''_{i-1}(k)$, the channel estimate is updated as $\hat{H}_{\text{CDP},i}(k) = \hat{H}'_{\text{CDP},i}(k)$.

Again, the first data symbol of the package, $\hat{H}_{\text{CDP},i-1}$ corresponds to the LS estimation. It is clear from the previously described process that the updating on the channel estimate is done starting on the second symbol of the package. The first symbol of the package is equalized as it was done in (10).

E. Frequency Linear-averaged Data Pilot decision-directed Estimation

Frequency Linear-averaged Data Pilot decision-directed Estimation (FLDP) was proposed in [12], and it is basically based on a combination of the STA scheme and the CDP method. First, it follows the STA algorithm, equations (10) to (13), and then executes the comparison process of the CDP scheme given by (15) and (16), using the same criteria for updating the channel estimate for the next symbol.

F. Time domain Reliable test Frequency domain Interpolation

Time domain Reliable test Frequency domain Interpolation (TRFI) is a mixed time-frequency domain estimation technique [13]. It follows up the same process of CDP the estimation, but it generates two sets of carriers: reliable and un-reliable. Reliable carriers are the ones that fulfill the criteria on the CDP update, whereas un-reliable carriers are the ones that do not fulfill the criteria. Instead of using the previous channel estimate for un-reliable carriers, it uses interpolation in order to calculate the channel response for these un-reliable carriers. As in [13], in this manuscript we use the spline cubic interpolation method for the interpolation process.

IV. Simulation Results and Discussion

In this section, and in order to analyze the performance of the channel estimation techniques in the IEEE 802.11p standard, we simulated the Geometry-Based Statistical Modeling (GBSM) non-WSSUS channel presented on [8] and the traditional stationary Rayleigh channel model. A single ring of interfering objects (IOs) that surrounds the R_X it is also assumed. In Table I common system parameters for T_X and R_X are given. Whereas in Table II particular system parameters for T_X and R_X are given. In table II, γ_T and γ_R are chosen in order to emulate two vehicles that circulate in two streets that intersect in a point.

TABLE I
Common System Parameters

Parameter	Variable	Value
Modulation	-	64-QAM
Bandwith	B	10 MHz
Carrier Frequency	f_c	5.9 GHz
OFDM Carriers	N_p	64
Training Symbols	T_{sym}	2
Data Symbols	D_{sym}	32
Initial distance between T_X and R_X	D	500 m
R_X IO ring radius	d	30 m

TABLE II
Particular System Parameters

	Transmitter		Receiver	
Parameter	**Variable**	**Value**	**Variable**	**Value**
Velocity	$\mathbf{v}_T$	40 km/h	$\mathbf{v}_R$	40 km/h
Azimuth Angle	γ_T	60°	γ_R	120°

Figure 3 shows the BER performance for the estimators described on section III. Monte Carlo simulations were performed with packages consisting on training and data symbols consistent with the parameters given in Table I. Figure 3 shows that time-domain based estimators, i.e., the estimation is only based on previously sent OFDM symbols (MSTA and CDP), are the ones that obtain better performance based on BER. The LS estimator is also a time-domain based estimator, but given its simplicity, it can be seen that it gives a worst performance. Nonetheless, the LS estimator has a better performance than the STA and TRFI estimators, which are both based on time and frequency domain (its estimation is based both on previously sent OFDM symbol and adjacent OFDM carrier frequency response).

For comparison purposes, Fig. 4 shows the performance of estimators based on both time and frequency domain, whereas Fig. 5 shows the BER performance of estimators based only on time domain. Figures 4 and 5 exhibit the performance for the stationary and non-stationary channel model presented in Section II. Figure 4 shows that time-frequency domain based estimators achieve considerably a better performance on the stationary case. For both stationary and non-stationary models, FLDP achieved the best performance. Also, for both stationary and non-stationary models, STA and TRFI estimators exhibit a similar performance for low E_b/N_0 regimes, but for higher values of E_b/N_0, TRFI outperforms the STA estimator.

Several facts are interesting to analyze in Fig. 4. The first one is that the STA estimator radically improves its performance on the stationary case. This result indicates that the linear averaging process performed on the STA estimator drastically degrades the performance of the estimator on the non-stationary case (a highly frequency selective channel).

Two comparisons are also interesting to point out. First, between STA and TRFI, techniques that rely on adjacent OFDM carrier frequencies. As TRFI uses spline cubic interpolation, which is more complex than a simple averaging process, it achieves a better channel estimation. The second

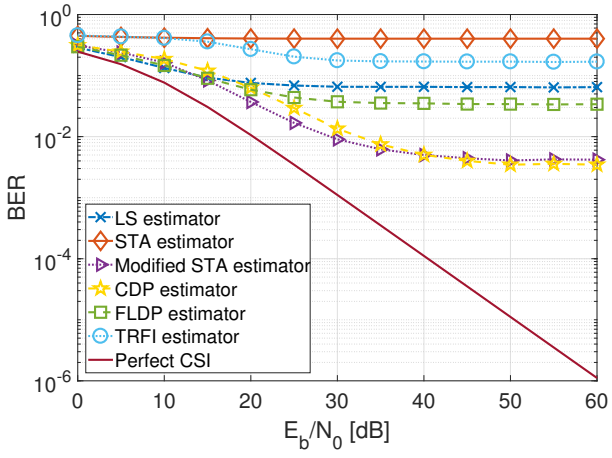

Fig. 3. BER performance for different estimators.

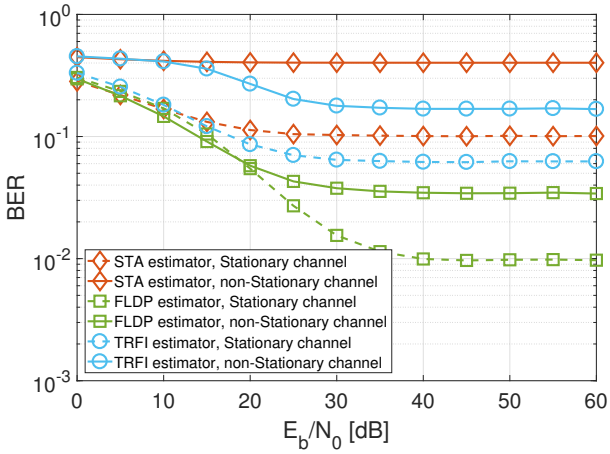

Fig. 4. BER performance for time and frequency domain based estimators.

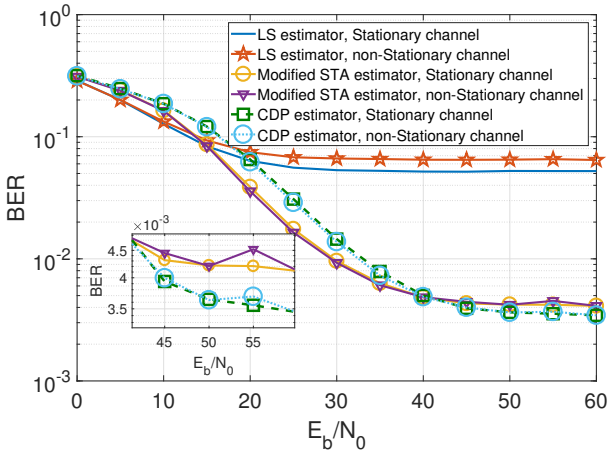

Fig. 5. BER performance for time based only estimators.

interesting comparison is between FLDP and TRFI because both techniques employ time and frequency estimation, but in a different order. TRFI first performs a carrier-by-carrier comparison, as in CDP, and later uses an interpolation operation for the non-reliable carriers. In other words, a time-domain estimation followed by a frequency-domain estimation is done. Further, FLDP performs the same adjacent frequency operation as STA, followed by the carrier-by-carrier comparison process of the CDP estimator (a frequency-domain estimation followed by a time-domain estimation). It can be seen that a time-domain estimation performed after a frequency-domain estimation achieves better performance than a frequency-domain estimation performed after a time-domain estimation. This was the case for the FLDP estimator, which outperforms the TRFI estimator.

Finally, Fig. 5 shows that the performance of the time based only estimators is not quite affected by the non-stationary condition of the vehicular channel. Nonetheless, a better performance is achieved by the LS estimator on the

stationary channel. Figure 5 also shows that the CDP and MSTA estimators exhibit a very similar performance both on stationary and non-stationary conditions. However, CDP performs a better estimate for high E_b/N_0 regimes. MSTA and CDP outperform the results of the LS estimator for high E_b/N_0 regimes, on both stationary and non-stationary conditions, as a result of the non-dynamically updating nature of the LS estimator.

V. Conclusion

In this paper, several novel proposed channel estimation techniques were evaluated both on a stationary and a non-WSSUS vehicular channel environment in terms of BER. It was shown that channel estimation techniques that take into account both the previously sent OFDM symbol and adjacent OFDM carriers, are not well suited for a non-WSSUS channel model. This is consistent with the empirical findings of the reviewed literature, that states that an IEEE 802.11p packet may exceed the stationary time of the vehicular environment, resulting in a highly time-dispersive channel (strongly frequency selective). On the other hand, the only time-based techniques analyzed in this manuscript achieved a better performance for the GBSM non-WSSUS analyzed channel, showing that these estimators are not affected by the non-stationarity of the channel. For E_b/N_0 regimes lower than 20 dB, both MSTA and CDP estimators outperform the LS estimator. It is also remarkable that the MSTA estimator has a gain of almost 5 dB for error probabilities between 10^{-1} and 10^{-2}.

Acknowledgment

The authors acknowledge the financial support of the Project "RETRACT" ERANet-LAC Grant No. ELAC2015/T10-0761 and Project FONDECYT Iniciación Grant No. 11160517.

References

[1] F. Qu, F. Y. Wang, and L. Yang, "Intelligent transportation spaces: Vehicles, traffic, communications, and beyond," *IEEE Communications Magazine*, vol. 48, no. 11, pp. 136–142, Nov. 2010.

[2] L. Li, D. Wen, and D. Yao, "A survey of traffic control with vehicular communications," *IEEE Transactions on Intelligent Transportation Systems*, vol. 15, no. 1, pp. 425–432, Feb. 2014.

[3] M. Awad, K. Seddik, and A. Elezabi, "Low-Complexity Semi-Blind Channel Estimation Algorithms for Vehicular Communications Using the IEEE 802.11p Standard," *IEEE Transactions on Intelligent Transportation Systems*, vol. PP, no. 1, pp. 1–10, May 2018.

[4] Z. Zhao, X. Cheng, M. Wen, B. Jiao, and C.-X. Wang, "Channel Estimation Schemes for IEEE 802.11p Standard," *IEEE Inteligent Transportation Systems*, vol. 5, no. 4, pp. 38–49, Winter 2013.

[5] M. Medard, "The effect upon channel capacity in wireless communications of perfect and imperfect knowledge of the channel," *IEEE Transactions on Information Theory*, vol. 46, no. 3, pp. 933–946, May 2000.

[6] L. Bernadó, T. Zemen, F. Tufvesson, A. F. Molisch, and C. F. Mecklenbräuker, "The (in-) validity of the WSSUS assumption in vehicular radio channels," in *2012 IEEE 23rd International Symposium on Personal, Indoor and Mobile Radio Communications - (PIMRC)*, Sept 2012, pp. 1757–1762.

[7] A. Roivainen, P. Jayasinghe, J. Meinila¨, V. Hovinen, and M. Latva-aho, "Vehicle-to-vehicle radio channel characterization in urban environment at 2.3 GHz and 5.25 GHz," in *2014 IEEE 25th Annual International Symposium on Personal, Indoor, and Mobile Radio Communication (PIMRC)*, Sept. 2014, pp. 63–67.

[8] C. A. Gutiérrez, J. T. Gutiérrez-Mena, J. M. Luna-Rivera, D. U. Campos-Delgado, R. Velázquez, and M. Pätzold, "Geometry-Based Statistical Modeling of Non-WSSUS Mobile-to-Mobile Rayleigh Fading Channels," *IEEE Transactions on Vehicular Technology*, vol. 67, no. 1, pp. 362–377, Jan. 2018.

[9] M. Engels, *Wireless OFDM systems: How to make them work?* Springer Science & Business Media, 2002.

[10] J. J. J. Rodriguez, "Modeling , Analysis , and Simulation of non-WSSUS Vehicle-to-Vehicle Channels," Ph.D. dissertation, Universidad Autónoma de San Luis de Potosí, San Luis de Potosí, 2018.

[11] J. A. Fernandez, K. Borries, L. Cheng, B. V. K. V. Kumar, D. D. Stancil, and F. Bai, "Performance of the 802.11p physical layer in vehicle-to-vehicle environments," *IEEE Transactions on Vehicular Technology*, vol. 61, no. 1, pp. 3–14, Jan. 2012.

[12] Y. Ren, D. C. Park, and S. C. Kim, "A novel channel estimation scheme for IEEE 802.11p in VANET," in *2015 Seventh International Conference on Ubiquitous and Future Networks*, July 2015, pp. 435–437.

[13] Y.-K. Kim, J.-M. Oh, Y.-H. Shin, and C. Mun, "Time and frequency domain channel estimation scheme for IEEE 802.11p," in *17th International IEEE Conference on Intelligent Transportation Systems (ITSC)*, Oct. 2014, pp. 1085–1090.

[14] J. A. Fernandez, D. D. Stancil, and F. Bai, "Dynamic channel equalization for IEEE 802.11p waveforms in the vehicle-to-vehicle channel," in *2010 48th Annual Allerton Conference on Communication, Control, and Computing (Allerton)*, Sept. 2010, pp. 542–551.